# Integrated, variablereluctance magnetic minimotor

by E. J. O'Sullivan

E. I. Cooper

L. T. Romankiw

K. T. Kwietniak

P. L. Trouilloud

J. Horkans

C. V. Jahnes

I. V. Babich

S. Krongelb

S. G. Hegde

J. A. Tornello

N. C. LaBianca

J. M. Cotte

T. J. Chainer

The use of lithography and electroplating to fabricate variable-reluctance, nearly planar. integrated minimotors with 6-mm-diameter rotors on silicon wafers is described. The motors consist of six electroplated Permalloy® horseshoe-shaped cores that surround the rotor. Copper coils are formed around each core. The Permalloy and copper electroplating baths, electroplating seed layers, and through-mask plating techniques are similar to those used to fabricate inductive thin-film heads. High-aspect-ratio optical lithography or X-ray lithography was used to form the various resist layers. The rotors were fabricated separately, released from the substrate, and then slipped onto the shaft, which was plated as part of the stator fabrication process. The fabrication processes for stator and rotor are described in this paper, and initial minimotor operation data are presented.

## Introduction

MEMS (microelectromechanical systems) encompasses the design and fabrication of miniature structures and systems such as sensors, actuators, controllers, and pumps in

applications ranging from aerospace technology to biotechnology. MEMS uses processing common in integrated microelectronics, but MEMS devices are three-dimensional devices with high aspect ratios and large structural heights, in contrast to essentially two-dimensional microelectronic devices. The first major commercial MEMS success was the Si-based pressure sensor in automobile air bags.

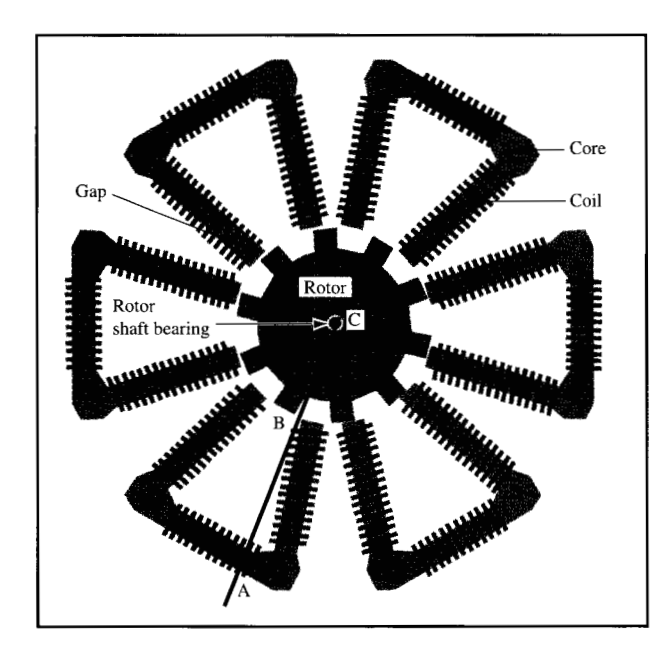
Various technologies are required for MEMS fabrication. Silicon structures are formed by bulk Si machining using wet or dry processes or by surface micromachining. Metallic "micromolding" techniques are also commonly used for fabrication of MEMS structures.

The most common micromolding technologies are photolithographic processes. Molds are created in polymer films, usually photoresist, on planar surfaces and then filled by electrodepositing metal. An important subset of MEMS is the rapidly emerging field known as Hi-MEMS, which uses X-ray lithography to create trenches up to 1 mm deep in polymethyl methacrylate (PMMA) resist on an electroplating base (called a seed layer). Electrodeposition of magnetic materials has made the formation of magnetically actuated devices possible in Hi-MEMS and in various areas of MEMS applications.

An important factor in the rapid growth of MEMS is the ability to use existing microelectronics fabrication

Copyright 1998 by International Business Machines Corporation. Copying in printed form for private use is permitted without payment of royalty provided that (1) each reproduction is done without alteration and (2) the Journal reference and IBM copyright notice are included on the first page. The title and abstract, but no other portions, of this paper may be copied or distributed royalty free without further permission by computer-based and other information-service systems. Permission to republish any other portion of this paper must be obtained from the Editor.

0018-8646/98/\$5.00 © 1998 IBM



Drawing of the variable-reluctance magnetic minimotor. The arrows trace one of the magnetic flux circuits in the operating minimotor. Line through stator shows location of cross section used in Figure 2 drawings.

technologies. IBM has long been involved in the development of silicon device fabrication, anisotropic etching of Si and thin films, and magnetic head fabrication. These technologies make use of optical, e-beam, and X-ray lithography, electroplating through patterned photoresist, electro-etching and lift-off, and related fabrication, packaging techniques, and equipment, all of which are applicable to MEMS.

As a step in developing the ability to build high-aspectratio structures using plating-through-mask technology, a rotary variable-reluctance electromagnetic minimotor was fabricated. In electronics, such a motor could find applications in small-diameter digital magnetic storage disk files with applications to digital high-resolution still photography and video. In addition, it would find applications in automotive, aerospace, biomedical, and military areas in the form of data storage, actuators, pumps, liquid distributors, and gyroscopes. When driven by means other than electrical power, the same structure could be used in microturbines and micropower generators.

This paper reviews IBM's work on the fabrication of magnetic minimotors. A description of the fabrication of a minimotor using optical lithography is followed by minimotor electrical test results. A first-pass motor was built using optical lithography to gain an understanding of the processing issues. A new minimotor stator design was then fabricated with X-ray lithography to enable more vertical walls and thicker structures.

# Minimotor operation

Shown schematically in Figure 1 is a minimotor consisting of a 12-pole stator and a 10-pole rotor.<sup>2</sup> The stator is a batch-fabricated multilayer structure containing horseshoeshaped magnetic cores<sup>3</sup> [1] with integrated Cu windings. The rotor is a patterned magnetic element that is fabricated separately and placed on a shaft located at the center of the stator assembly. The stator design minimizes the magnetic flux path by employing horseshoe-shaped cores, each of which forms a complete magnetic circuit with the rotor to reduce magnetic path length. An active magnetic circuit for one core of the minimotor is outlined with arrows in Figure 1. The motor has three phases, produces a 12° rotation per stroke,<sup>4</sup> and requires 30 strokes per revolution. The motor works as follows: When a stator core is energized, it pulls the nearest rotor tooth (pole) into alignment with its poles; this causes the other rotor teeth to be misaligned relative to the other stator cores, because there are 12 stator poles and only 10 rotor teeth. Energizing the next stator core turns the rotor an additional 12°. By energizing the stator cores in succession, a continuous rotation of the rotor can be achieved. In a simple magnetic circuit model, the torque (T) varies as the square of the magnetomotive force (Ni)applied by the coils; it depends on pole height, i.e., core thickness (h), at the stator-rotor gap (g) and rotor radius (r) as follows [2, 3]:

$$T = \left[\frac{1}{2}\,\mu_0(Ni)^2 hr\right] / g,\tag{1}$$

where  $\mu_0$  = permeability.

# Optically fabricated minimotor

# • Minimotor processing sequence

The key physical parameters of the optically fabricated minimotor are given in **Table 1**. The fabrication sequence for the stator (Figure 2) used a series of lithographic and

<sup>&</sup>lt;sup>1</sup> In a magnetic circuit, reluctance is the analog of resistance in an electric circuit.

<sup>&</sup>lt;sup>2</sup> Rotating electrical machines consist of a stator and a rotor (the moving part) separated by a small air gap. The stator contains current-carrying windings around a magnetic core; in macroscopic motors the rotor may also contain windings.

<sup>&</sup>lt;sup>3</sup> A core is also known as a yoke.

<sup>&</sup>lt;sup>4</sup> The distance the rotor travels when a stator core is energized is known as a stroke.

<sup>&</sup>lt;sup>5</sup> Magnetomotive force, the product of the current (i) times the number of coil turns (N), is the analog of voltage in an electric circuit.

<sup>&</sup>lt;sup>6</sup> The permeability is analogous to conductivity in an electric circuit. However, magnetic circuit models are not as good approximations as electrical circuit models, since the permeability of soft ferromagnetic material is much lower than the conductivities of practical conductors. Consequently, magnetic flux may not be confined within the magnetic circuit boundaries, and magnetic flux leakage may have a deleterious impact on performance.

electroplating steps similar to those in thin-film head manufacturing [4] and in the fabrication of micromachined inductors [5, 6]. The process for the stator began by sputter-depositing a Ti/Cu/Ti seed layer on an oxidized Si wafer, lithographically forming the "plate-through" (patterned) mask for the bottom part of the windings, removing the upper Ti layer, and electroplating Cu in the exposed seed layer regions [Figure 2(a)]. The resist and seed layer were then removed from the regions between the electroplated features, a polymer dielectric was applied across the entire structure, and the surface was planarized [Figure 2(b)]. A thin patterned polymer dielectric was formed on top of the Cu to insulate the windings from the magnetic core, leaving apertures at the end of each copper bar to permit formation of a coil in the subsequent steps [Figure 2(c)]. A second seed layer of Ti/Cu/Ti was deposited, a resist pattern was formed, the upper Ti was etched away, and Permalloy\*\* (80 at.%/20 at.% Ni/Fe alloy) was electroplated [Figure 2(d)]. Following the removal of the resist and seed layer, the Permalloy core was surrounded by dielectric [Figure 2(e)]. The top elements of the winding were formed using similar process steps [Figures 2(f), 2(g)], making connections between the upper level and the lower level of the winding through the previously mentioned apertures in the thin dielectric [Figure 2(f)]. To simplify fabrication, the studs that join each turn of the coil were electroplated with Permalloy at the same time that the magnetic core was being electroplated. The structure can be encapsulated by a final polymer dielectric application [see Figure 2(h)].

The rotor was fabricated by electroplating Permalloy on a separate lithographically patterned Si/SiO<sub>2</sub> substrate precoated with a 1- $\mu$ m-thick layer of Cu (the usual adhesion layer under the Cu was Ti or Ta). The rotor was detached by chemical dissolution of the Cu layer and slipped onto the shaft located in the center of the cavity that had been opened in the stator [Figure 2(h)]. The rotor shaft and rotor-support pins were formed during the same lithographic and electroplating steps that were used to create the cores and windings [see Figure 2(a)].

# Seed layers

Seed layers for Cu and Permalloy electrodeposition consisted of sputtered Cu (1000–3000 Å) on either a Ti or Ta adhesion layer. A layer of Ti was usually deposited on the Cu to enhance resist adhesion. In the case of Permalloy electrodeposition, a 1000–2000-Å sputtered Permalloy layer without an adhesion layer was occasionally used.

# • High-aspect-ratio optical lithography

The minimotor fabrication process was initially developed using high-aspect-ratio optical lithography. In the process

 Table 1
 Minimotor parameters.

	radius		Coil conductor width (µm)	Gap between coil conductors (µm)	Air gap between rotor and stator (µm)	Coil turns (per core)
17	2976	700	60	30	5-40	108

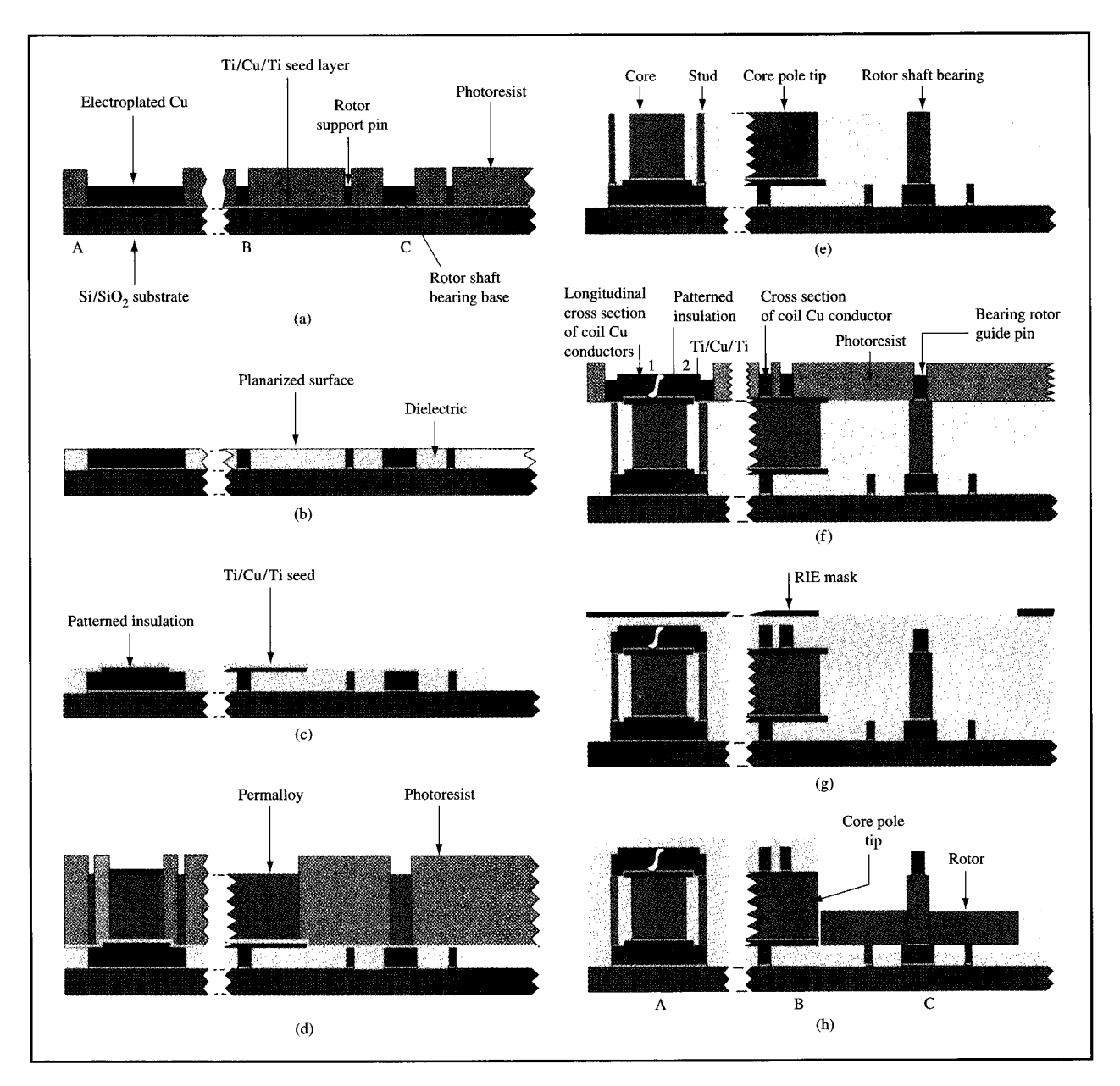
we investigated how far optical resists could be extended to thick patterns with high aspect ratios. Both positive (novolac-type) and negative optical resists were employed. Although the positive resists are more attractive because of ease of removal following electrodeposition, they are more difficult to process at large thicknesses, e.g., with respect to sidewall angle.

The principal negative resist consisted of solutions of various concentrations of Shell EPON\*\* Resin SU-8, prepared [7] and photosensitized with a commercially available triaryl sulfonium salt, such as CYRACURE UVI\*\* from Union Carbide Corporation. With this resist, near-vertical sidewall profiles (85–90°) were obtained for a range of resist thicknesses up to 140  $\mu$ m for single layers of resist on copper and Permalloy seed layers.

The positive-working resist, a high-viscosity novolac obtained from Shipley (SJR\*\* 3740) or Hoechst Celanese Corporation (AZ\*\* P4620), was applied using a multilayer spin method to achieve thicknesses of up to 70  $\mu$ m. This resist could be exposed using UV light, and was readily removed without affecting the underlying structure. Hexamethyl disiloxane (HMDS) was used to obtain good adhesion of the resist to the underlying electroplating Cu seed layer. A baking procedure was necessary to stabilize the resist prior to UV light exposure. Resist patterning was achieved using contact printing with the aid of a standard UV mask aligner (Karl Suss). Resist patterns were developed in a commercially available alkaline-type developer. A single UV exposure step was employed to pattern the resist layer. Reasonably straight sidewalls were obtained for resist up to 50 µm thick.

#### Electrodeposition of magnetic material

The rotors and the stator cores [Figure 2(d)] were made of Permalloy (the stator's second level of metallurgy), an electroplated material that is magnetically soft [8, 9]. For convenience of fabrication, the same electrodeposition step was used to generate the middle section of the winding vias, as well as the main body of the pin (Figure 2). Deposition was carried out in a horizontal paddle cell [10, 11], with the paddle between the electrodes traveling the length of the cell at a frequency of 60 Hz and a height of about 3 mm from the cathode surface. The plating cell



#### Webster Co.

(a) Start of schematic representation of step-by-step fabrication of the minimotor stator. The cross section used is that represented by line A-C in Figure 1, and includes cross sections of the rear section (A), a portion of the core near the pole-gap region (B), and the rotor shaft bearing in the middle of the stator (C). The figure shows the electroplated Cu layer on a Ti/Cu seed layer in the resist pattern (the exposed Ti layer was removed by etching prior to electroplating). (b) After removal of resist and seed layer from between the electroplated Cu features, the structure was backfilled with epoxy dielectric and polished to planarize and expose the tops of the Cu features. (c) Shown is the patterned layer that insulates the bottom Cu coils from the Permalloy core along with a layer of Ti/Cu/Ti electroplating seed layer. (d) This shows the electroplated Permalloy layer in the resist pattern. Note that the as-deposited core is higher than the vias by an amount equal to the thickness of the patterned insulation layer (assuming good electroplating uniformity). (e) Following removal of the resist and seed layers from between the electroplated Permalloy features, the structure was backfilled with epoxy dielectric and polished to planarize and expose the tops of the Permalloy features. (f) After applying and patterning the second insulation layer required to insulate the Permalloy core from the top Cu coil conductor level, a third electroplating seed layer and photoresist were applied, and the top Cu layer was electroplated. Top Cu conductor segments 1 and 2 belong to adjacent windings within the spiral coil around the Permalloy core. (g) The resist and seed layers were removed from between the Cu features, a layer of insulation was applied, and an RIE mask was patterned to expose the rotor cavity in the middle of the stator and Cu pads for wire bonding. (h) The completed minimotor structure shown after RIE of the rotor cavity in the stator. The rotor is shown at rest on the rotor pin supports. Locations A–C are

was connected to a larger plating-solution reservoir. The solution was continuously filtered using 0.2-μm filters (Millipore\*\* Corporation). The plating reservoir was equipped with an automatic temperature-control system, used to stabilize the temperature at  $27 \pm 0.1$ °C. The solution pH was controlled at  $3 \pm 0.1$  through automatic addition of HCl solution (as needed). Separately, using a Brinkmann Instruments Dosimat, the ferrous ion concentration was kept constant by adding a ferrous sulfate solution (pH = 2) at a rate calculated to match the rate of iron consumption. A nickel plate served as the anode, and a stainless-steel plate surrounding the cathode served as an auxiliary electrode [11, 12]. The auxiliary electrode, which is often called a "thief," is coplanar with the cathode. The auxiliary electrode reduces "current crowding" at the edge of the cathode and hence improves deposit thickness uniformity across the cathode, especially near the edge. The magnitude of the current that must be passed through the auxiliary electrode depends on the current density at the cathode [11, 12].

The current densities used were in the 5.1–9.1-mA/cm<sup>2</sup> range (calculated for the active area on the wafer). On the basis of work by Mehdizadeh et al. [12–14], auxiliary electrode current densities were set at 1.1–1.2 times the superficial wafer current densities. As a result, deposit height was uniform across the wafer. Individual features, however, did exhibit some nonuniformity of the "rabbitears" type (i.e., increased thickness at the metal–resist boundary). The increased rate of growth was particularly noticeable in larger features surrounded by a large area of resist, such as the rotor edges and the stator pin. This behavior is as predicted by the model [13]. Where necessary (in the case of the stator), the Permalloy layer was planarized by polishing.

# • Electrodeposition of copper

Electroplated Cu was used for the bottom and top portions of the conductor coils, for the rotor supporter pins, and for the top portion of the rotor shaft [Figure 2(a)]. Electroplating from a commercially available, acid—Cu plating solution was carried out in a paddle cell [8, 11]. The plated Cu was fine-grained and bright and, like plated Permalloy, faithfully reproduced the shape of the photoresist pattern.

The Cu thickness was uniform on the feature scale. The uniformity on the stator scale was governed by the layout of the elements to be plated; isolated features generally were thicker than those surrounded by other features. The across-wafer uniformity was good when there was a large peripheral region to serve as an on-wafer current "thief."

# • Dielectric materials and planarization

Dielectrics for MEMS structures must exhibit low stress and be planarizable. Various dielectric materials including polyimide, hard-baked photoresist, and epoxy resin were investigated for insulating and planarizing the various levels of the minimotor. The use of polyimide necessitated the use of a barrier layer, e.g., an electrolessly deposited material such as Ni(P), to prevent a chemical reaction with Cu during polyimide curing. In addition, voids formed due to the difficulty of removing solvent from the deep, narrow recesses resulted in numerous shorts between the coils and the magnetic core. A proprietary solventless epoxy resin not only eliminated the problem of voids but also reduced stress, since it did not require curing at high temperatures (the temperature normally used for polyimides ranges from 350 to 400°C). The cured epoxy dielectric was polished to planarize the surface and to expose either the Cu [Figure 2(b)] or the Permalloy features [Figure 2(e)]. Polishing was carried out using a Strasbaugh polishing tool and vendor-provided polishing pads and silica slurries.

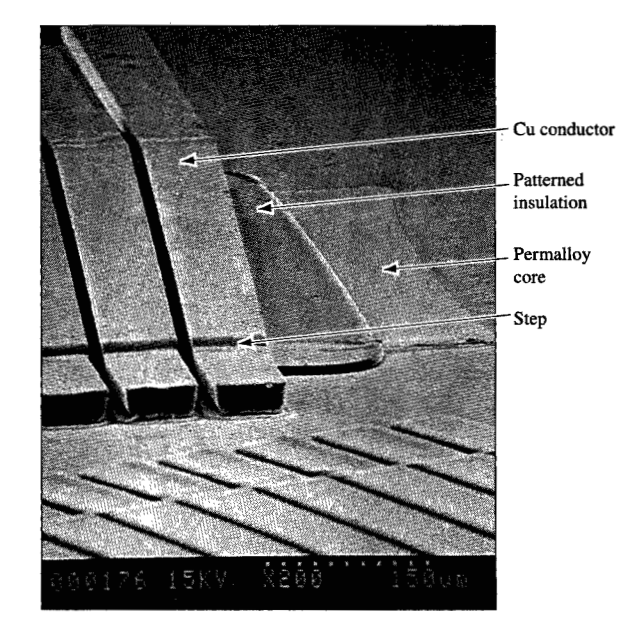
# Interlevel insulation layer

This insulation is important in the motor fabrication process because it isolates the magnetic core from the bottom and top Cu conductors. There are various ways to approach fabrication of this level; the one chosen here was to spin-coat the planarized substrate with a 5-7-µm-thick layer of epoxy. The epoxy was then patterned, leaving behind a band of epoxy that covered all but the ends of the Cu conductors for stud connections for the bottom coil conductors [Figure 2(c)]. After curing of this insulation layer, a seed layer was deposited, followed by photoresist. Although this insulation layer created a nonplanar surface, this was not a problem for subsequent resist processing. The difference in height between the core and the studs after Permallov electrodeposition was removed by the polishing step following epoxy backfill. An approach similar to that shown in Figure 2(c) was employed to coat the exposed polished Permalloy core, leaving the vias bare prior to fabrication of the top Cu conductor layer of the minimotor.

# Process integration and completion of the minimotor structure

Stators were completed with 30-34- $\mu$ m-thick Cu conductors and 40-45- $\mu$ m-thick Permalloy cores using optical lithography. The final structure required five mask levels [excluding the masking required for reactive ion etching (RIE) of the rotor cavity at the end of the fabrication process] and three levels of electrodeposited metal. The minimotor required a Permalloy layer greater than 25-30  $\mu$ m in thickness to achieve rotor levitation and

685



Top view of a pole-tip region of a completed Permalloy core showing the topmost regions of the Cu coil conductors, the patterned insulation layer insulating the Permalloy layer and the top of the Cu coil, and the Permalloy core tip.

develop a torque sufficient to overcome friction. The Cu layer had only to be thick enough to carry current without undue heating, and was therefore kept fairly thin to reduce stresses that build up in thick structures. Figure 3 is an SEM side view of a completed stator core prior to opening the rotor cavity. In this figure one can see the Permalloy core pole-tip region, the exposed portion of the second, or upper, patterned insulation layer, and the top Cu coil conductors. Also evident in the Cu conductors are the "steps" associated with the edges of the patterned insulation layer.

The rotor cavity in the stator was opened using RIE, with masking to ensure selectivity; epoxy dielectric removal rates were  $\sim 0.5~\mu m$  per minute. The RIE tool, a Leybold Z401 model, employed a water-cooled stage; a thermally conductive compound was placed between the sample and the stage. To avoid excessive heating and structural damage, runs were interrupted periodically. Figure 4 shows a section of a completed and assembled motor.

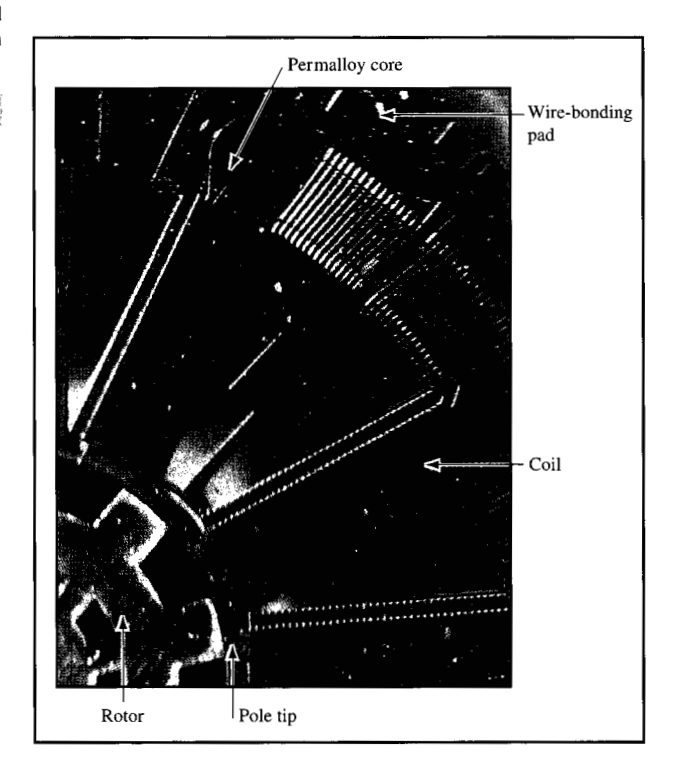
Process integration was key to completion of the minimotor. Factors that required attention included a) minimization of heating during sputter deposition of the electroplating seed layer to, e.g., prevent void formation at the Cu conductor/dielectric interface, which caused cracks

and voids in the thin insulation layer between the bottom Cu conductor layer and Permalloy; b) dielectric-related problems such as voids and coefficient of thermal expansion (CTE) mismatch; c) minimization of heating during the RIE step used to open the rotor cavity in the stator; and d) ensuring that solvents and solutions used in processing subsequent layers did not interact with underlying layers.

## • Modeling and testing

A lumped-parameter computer model [2] was developed to explore the design space of several independent motor parameters including rotor/stator radius ratio, stator-rotor field gap, stator magnetic core thickness, core permeability, coil-packing fraction, and saturation flux density. This design space allowed us to arrive at the design point used for the minimotor. A 3D magnetostatic model [3] that takes into account all of the significant flux paths was subsequently used to estimate the magnetic performance of the motor.

Figure 5 shows torque versus thickness of the magnetic layer. The two curves are the result of the lumped-parameter model [2] and of the 3D magnetostatic



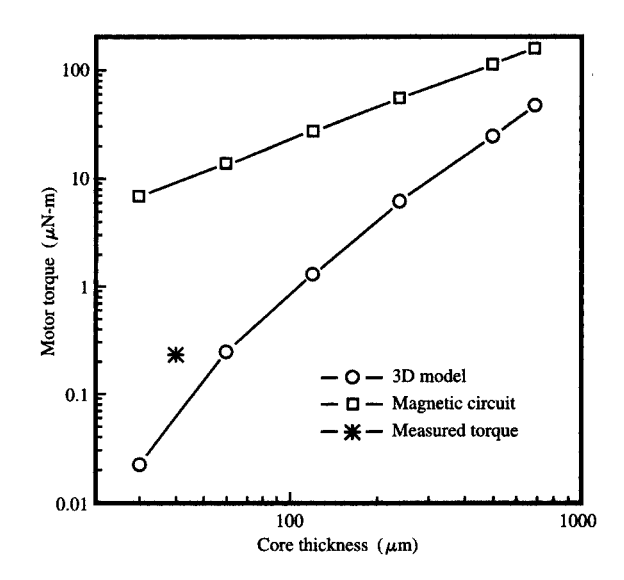
Top view of a section of a completed and assembled minimotor showing portions of several Permalloy yokes and pole tips of a stator "wound" with 60-\mum-wide plated Cu coil. A Permalloy rotor is positioned on a shaft bearing.

computation [3]. In both cases, the current was adjusted for saturation of the magnetic material. It is clear from Figure 5 that the 3D computed torques at small magnetic core thicknesses are significantly lower than those predicted by the lumped-parameter magnetic circuit model. In the 3D model, a conservative value of 1000 was assumed for the relative permeability of the core. As the magnetic core thickness increases and the aspect ratio of the core increases, the flux losses decrease, and at a Permalloy thickness of  $\sim 1000 \mu m$  the torque values calculated using the two methods are nearly the same. Increasing the permeability of the magnetic material or reducing the length of the magnetic circuit (by reducing the motor diameter) improves the efficiency of the magnetic circuit, i.e., reduces flux leakage from the core in regions away from the gap.

Flux leakage reduces the fields in the gaps and, therefore, the achievable torque. According to Ampere's law, if the gap fields are reduced, the fields in the other parts of the magnetic circuit must be increased. As a result, local saturation of the magnetic circuit occurs at a lower current than would be predicted from the lumped-parameter model. If the Permalloy coil is operated below saturation, the torque reduction due to flux leakage is compensated by increasing the current at the expense of increased power loss (lower efficiency). Above saturation, a further increase in the current is not effective in increasing the torque.

The fabricated prototype minimotor (with overall dimensions given in Table 1) has the measured mechanical and electrical characteristics summarized in **Table 2**. The motor was driven open-loop, since it did not have a built-in feedback sensor to detect the rotor position. The motor torque as determined from the angular dependence of inductance is  $2.3 \times 10^{-7}$  N-m at 100 mA (zero to peak). This is indicated by the asterisk in Figure 5. The rotor levitation threshold is 60 mA.

In the open-loop configuration, maximum rpm is limited by the undamped resonance of the rotor. Torque, as determined from the dependence of the slope of the holding torque to the maximum rpm at a given current, is  $1.8 \times 10^{-7}$  N-m at 100 mA (zero to peak), which is in good agreement with the value derived from inductance variation. From Figure 5, it is seen that the measured motor torque is in reasonable agreement with the 3D model prediction. The lumped-parameter torque is much higher and has a linear dependence on the thickness of the magnetic core layer. The difference between the models is attributed to the reduced current to reach saturation of the magnetic core material and to the reduced magnetic potential drop across the gap. The inclusion of flux leakage and early magnetic saturation is important in the design of electromagnetic circuits



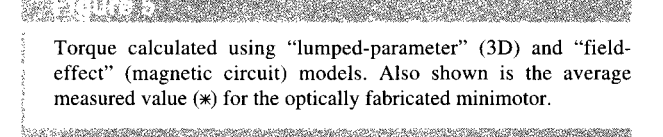
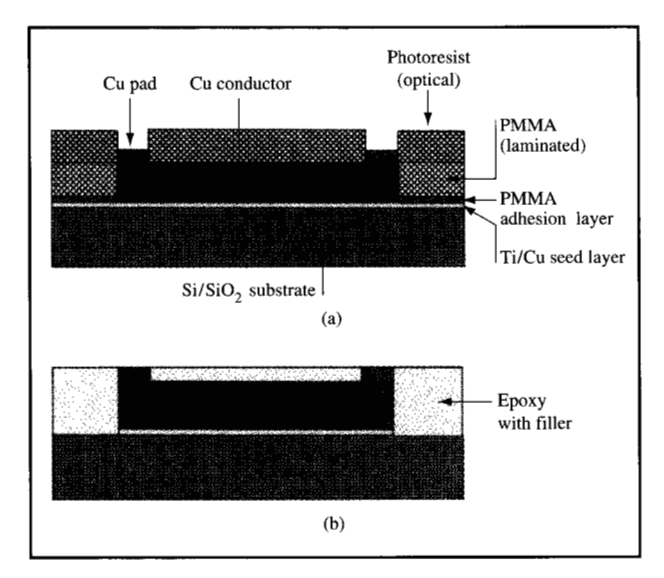


 Table 2
 Minimotor: Preliminary evaluation.

- Motor thickness values: Cu conductors 30–35  $\mu$ m; Permalloy 43  $\mu$ m; rotor 20  $\mu$ m.
- Field gap  $\approx 40 \mu m$ .
- Rotor-shaft clearance  $\approx 9-10 \mu m$ .
- Inductance per half phase (without rotor)  $\approx 19~\mu H$  (one horseshoe).
- Aligned inductance (one phase fully aligned)  $\approx 23 \mu H$ .
- Unaligned inductance  $\approx 20 \mu H$ .
- Static torque from angular dependence of  $L \simeq 2.3 \times 10^{-7}$  N-m.
- Rotor moment of inertia  $\approx 2.5 \times 10^{-11} \text{ kg-m}^2$ .

in micromechanical applications such as the planar minimotor studied here.

The modest torque is the result of using optical lithography to fabricate the stator. Although the rotor was fabricated using X-ray lithography, the less-than-90° sidewall angle exhibited by the optically patterned positive photoresist used for stator fabrication lowered the efficiency of the motor due to the large clearances between the stator and rotor pole tips and between the shaft and rotor. The friction caused by the few microns of eccentricity in the rotor–shaft interface further lowered the torque.



(a) Schematic representation of the process used for fabrication of the bottom Cu conductors and spacer pads in the minimotor built using X-ray lithography. A cross section along the length of a bottom Cu coil conductor is shown. This figure depicts the structure after electroplating the Cu spacer pads in an optical resist pattern after first electroplating the bottom Cu conductors in X-ray-exposed PMMA resist. (b) After removal of the X-ray PMMA and optical resists and seed layer from between the electroplated Cu features, the structure was backfilled with silica-filled epoxy dielectric and polished to planarize and expose the tops of the Cu features.

# Minimotor fabrication using X-ray lithography

From the experience gained with the optically patterned minimotor, the motor was redesigned to make the fabrication process easier and to improve motor performance by reducing magnetic flux leakage losses during operation. Elements in the design that were changed included 1) reducing the number of turns in the Cu coils in order to increase the conductor and via dimensions and spacings; 2) widening the stator cores in the regions away from the pole tips; 3) eliminating the coils in the rear of the cores in the optically fabricated minimotor, which were found not to contribute significantly to motor operation; and 4) increasing the number of openings in the rotor to facilitate solution access during the process of chemical release from the substrate. Four stators were placed in a 40-mm × 40-mm area<sup>7</sup> on a 4-in.-diameter oxidized Si wafer; three stators had 40 coil windings per core (i.e., 20 windings on each arm of the horseshoe-shaped core), and one had 20 coil

windings per core. The 40-winding coil had studs 100  $\mu$ m wide and 140  $\mu$ m long, and the 20-winding coil had studs 160  $\mu$ m wide and 200  $\mu$ m long.

The processing approach and the choice of materials were modified in order to use X-ray lithography in the fabrication of the newly designed stator. In the optical motor the photoresist for electroplating the magnetic-core and conductor vias was applied by spin coating. It therefore conformed to the nonplanar bottom conductor and magnetic core, which contained the 5-μm-thick patterned insulation layer. Since in the LIGA<sup>8</sup> process the semirigid PMMA sheet is glued to the substrate with PMMA 1-2 μm thick, which is spin-coated, it was necessary here to planarize the surface by polishing after each X-ray lithography step beyond the first. The development of a different method for isolating the magnetic core from the top and bottom conductors of the Cu coils was required.

#### Fabrication

Like the optically fabricated motor, the X-ray fabricated minimotor basically consisted of a bottom Cu level, a Permalloy magnetic core level, a top copper level, and insulation layers to isolate the Cu conductors from the core. Each of the three main metal levels was built by applying a Ti/Cu/Ti seed layer and spin-coating and thermally curing  $\leq 2~\mu m$  of the PMMA adhesion layer. "Gluing" a 1-mm-thick PMMA sheet (Perspex CQ), "flycutting" to thin the PMMA sheet to the desired thickness, usually about  $100-150~\mu m$ , and X-ray exposure were carried out at CAMD. These were followed by resist-pattern development, <sup>10</sup> pretreatment of the surface to remove Ti, electroplating Cu or Permalloy, and polishing the PMMA resist back to the metal features.

The process was continued by applying AZ optical resist, UV-exposing and developing the resist, and electroplating thin ( $\sim$ 20–25  $\mu$ m) Cu spacer pads [Figure 6(a)]. Figure 7 is a scanning electron micrograph of electroplated Cu spacer pads. The Cu lines in Figure 7 obtained from the X-ray-patterned resist exhibit vertical sidewalls and well-defined corners; the pad features are not as well-defined as the line because of the limitations of the optical lithographic process for thick-resist processing, as mentioned previously. Following removal of the AZ resist, PMMA, and seed layers (the latter by either chemical etching or ion milling), an epoxy dielectric with a silica filler was applied and thermally cured. The excess dielectric was removed by polishing to expose the

 $<sup>^{7}</sup>$  40 mm  $\times$  40 mm was the maximum area that could be conveniently scanned by the X-ray beam at the Center for Advanced Microstructures and Devices (CAMD) of Louisiana State University at Baton Rouge.

<sup>&</sup>lt;sup>8</sup> LIGA, a common acronym used in association with Hi-MEMS fabrication, is an abbreviation of the German phrase Lithographie, Galvanoformung, and Abformung (lithography, electroforming, and replication).

These two steps were carried out either at the MCNC (Microelectronics Center of North Carolina) or at the IBM Thomas J. Watson Research Center.

<sup>&</sup>lt;sup>10</sup> This step was carried out either at CAMD or at the IBM Thomas J. Watson Research Center.

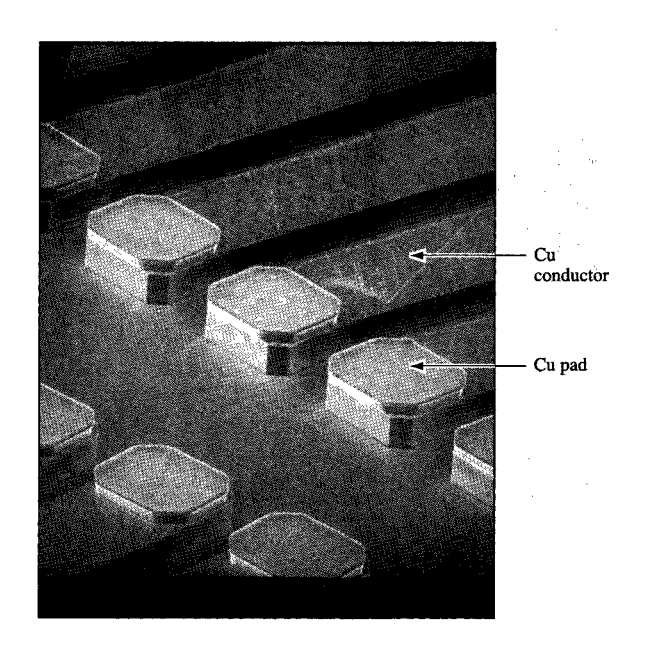
Cu features [Figure 6(b)] in preparation for the seed layer and X-ray lithography steps of the next level.

The above sequence was repeated to fabricate the Permalloy levels. As in the previous minimotor, the studs connecting the top and the bottom Cu conductors were made of Permalloy electroplated at the same time as the magnetic core. After polishing back the PMMA resist to the Permalloy features, Permalloy spacer pads  $\sim\!20\text{--}25~\mu\mathrm{m}$  high were electroplated on the Permalloy studs using optically patterned photoresist. Following encapsulation of the Permalloy features with silica-filled dielectric and polishing it back to the Permalloy features, the top Cu coil level was fabricated using X-ray-patterned PMMA resist. The rotor shaft was plated in stages each time a stator feature was plated.

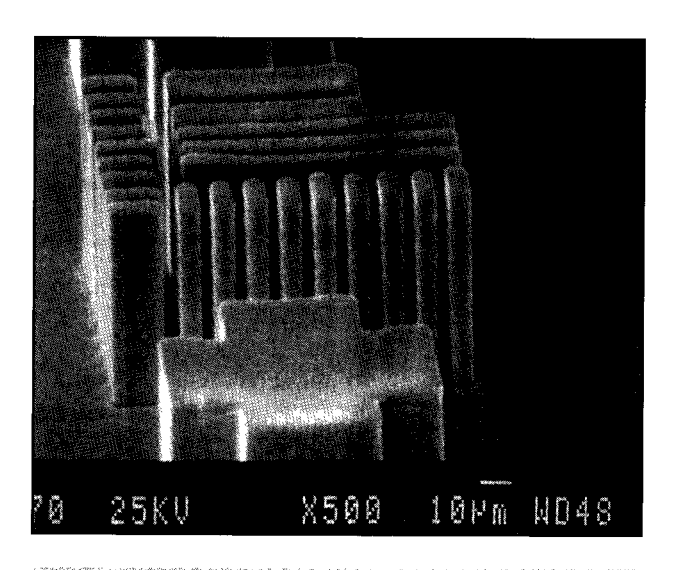
X-ray lithography provided vertical wall profiles, which are important for the rotor and stator core pole tips. An example, shown in **Figure 8**, of a Cu pattern electroplated through X-ray-patterned PMMA resist illustrates the capability of X-ray-patterned PMMA resist to provide high-aspect-ratio structures using thick resist with vertical sidewalls. The smallest features in this alignment-mark pattern are separated by  $\sim 5~\mu m$ . However, the simpler optical-resist-patterning process provided adequate definition for the metal pads ( $\sim 15~\mu m$  thick after polishing) for dielectric to be maintained between the upper and lower copper conductor windings and the Permalloy core.

Figure 9 is a scanning electron micrograph of a region near a stator pole tip following removal by RIE of most of the encapsulating silica-containing epoxy resin dielectric from the central rotor region. Because of mask undercutting during the RIE process, dielectric has been removed from the stator region for some distance back from the pole tip. The five-level structure in this picture consists of top Cu conductors, a portion of the front bottom Cu conductor, and the Permalloy studs, all three types of features fabricated using X-ray lithography. Also visible are parts of the Cu spacer pads on the ends of the bottom conductors and the Permalloy spacer pads on the Permalloy studs. Removal of the dielectric was carried out using SF<sub>6</sub>/O<sub>3</sub> gas. In contrast to the fabrication of the stator using optical lithography (Figure 4), the presence of silica filler in the dielectric of the present stator complicated the etching process, since the etch rate of the silica was less than that of the epoxy resin. Thus, the RIE process had to be periodically interrupted (notwithstanding cool-down interruptions) to allow manual removal of loosely attached silica on the surface of the receding dielectric.

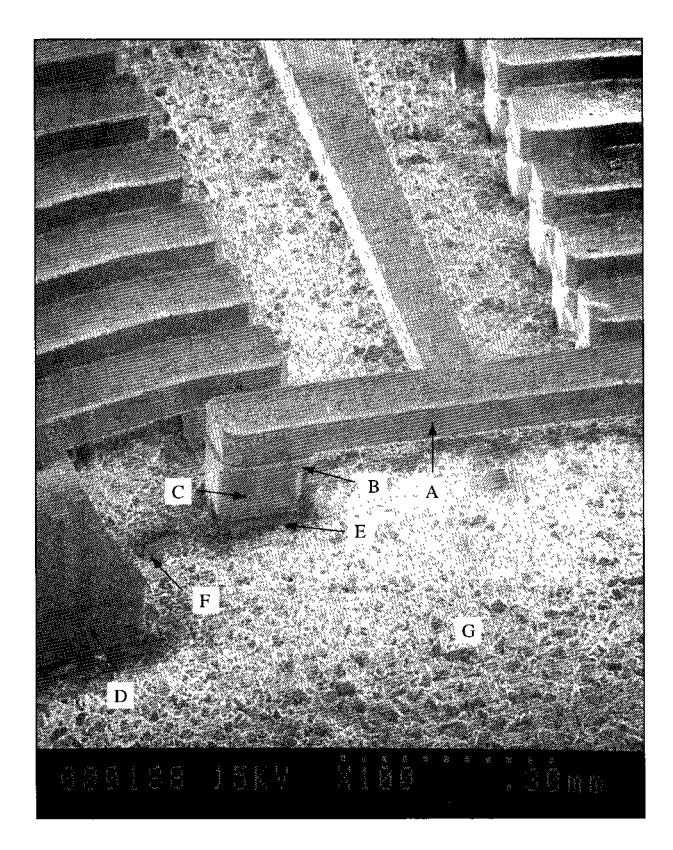
The rotors were electroplated on a separate substrate through X-ray-exposed PMMA, detached, and slipped over the integrated rotor-shaft bearing following RIE opening of the rotor cavity in the stator. An assembled minimotor



Scanning electron micrograph of Cu spacer pads electroplated using AZ optical photoresist on Cu bottom conductors that were electroplated using X-ray-patterned PMMA resist. Both resists were removed prior to taking the picture, but the Ti/Cu/Ti seed layer on the oxidized Si surface between the lower features was not removed.



Scanning electron micrograph of a lithographic alignment mark pattern of Cu electroplated through X-ray-patterned PMMA which was then removed. The smallest features are 7  $\mu$ m wide and 70  $\mu$ m high; the separation between these features is 5  $\mu$ m.



#### W. 14 3 3 4 3 4 3

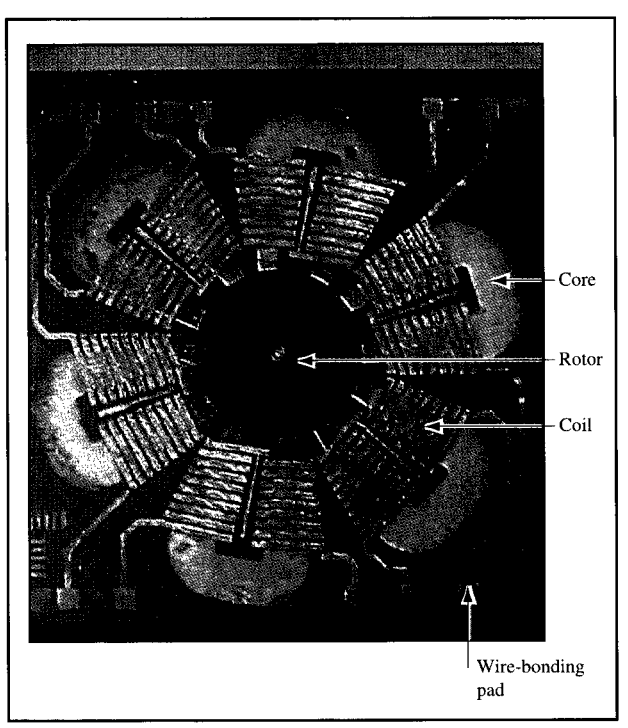
Scanning electron micrograph of a stator region between the two pole tips of a core (only one pole tip shown). A: top Cu conductor; B: Permalloy spacer pad; C: Permalloy stud; D: Permalloy core; E: Cu spacer pad; F: bottom Cu conductor only partially exposed in the RIE process; G: surface of remaining reactively ion-etched silica-filled epoxy resin dielectric. Features A, C, D, and F were electroplated using X-ray-exposed PMMA resist, while B and E were electroplated using optically exposed resist.

of the type with 20 windings per coil is shown in **Figure 10**. The rotor is 40  $\mu$ m thick, the stator Permalloy core 100  $\mu$ m thick, and the Cu conductors about 45  $\mu$ m thick. The minimotor is functional; however, testing has not been completed.

• Fabrication process compatibility with X-ray lithographic processing

The use of X-ray lithography, which allows fabrication of significantly thicker structures, poses certain challenges [15]:

 The thicker layers exacerbated thermal mismatch problems between windings in the copper coils, Permalloy core, and dielectric. The thermal mismatch in the vertical direction (perpendicular to the substrate) became a serious issue. A perfectly planarized layer



Top view of a completed minimotor with rotor in place. The stator was fabricated using three X-ray and two optical lithography steps, the rotor using X-ray lithography.

containing metal features embedded in a polymer, usually with high coefficient of thermal expansion, can suffer delamination at the vertical metal-polymer interface when heated to 180°C during curing of the spun-on PMMA, and can also cause cracking and delamination of the seed layer. This problem was eliminated by using a dielectric containing a low-CTE filler, silica.

- 2. Using a dielectric containing inorganic particles to reduce the CTE necessitated changes in the RIE process used to open the rotor cavity in the stator.
- 3. The 100-400-μm-thick PMMA created alignment problems because of the difficulty of accurately registering a mask to alignment marks under the thick resist. Techniques for alignment through PMMA up to 400 μm thick with ±5-μm accuracy were developed in a joint effort by MCNC, CAMD, and IBM [16]. The alignment entailed developing a jig that permitted optical alignment, clamping of the X-ray mask to the substrate, and forming windows in the resist to be able to see the specially designed alignment marks without distortion.

- 4. Successful plating of small features in the thick PMMA required special attention to the entire sequence of steps from the development of the PMMA through the plating operation. A high yield in plating, particularly of the 100-μm-wide and 140-μm-thick studs through the thick PMMA mask, was achieved by developing a sequence of surface pretreatment, PMMA development, and wetting initiation steps that ensured uniform onset of plating in all of the resist openings at the same time.
- 5. All solvents and chemicals used in PMMA processing had to be compatible with materials incorporated in the underlying structure.
- 6. Successful lamination of the PMMA sheet as described in the fabrication section above required that irregularities in the planarized wafer surface be minimized. Producing the required degree of planarization necessitated the development of appropriate polishing techniques to deal with the various composite surfaces at each level.

#### Conclusions

A batch-fabrication process using lithography, electroplating, dielectric filling, and planarization steps was employed to fabricate variable-reluctance magnetic minimotors using either all optical or mostly X-ray lithographic patterning. These motors were successfully operated and exhibited electrical integrity and magnetic functionality. For the optical minimotor with a Permalloy core thickness of 43  $\mu$ m and a rotor thickness of 20  $\mu$ m, a torque of 5 × 10<sup>-7</sup> N-m was measured.

The X-ray lithographically fabricated motor described in this work (100- $\mu$ m-thick Permalloy core with 40- $\mu$ m-thick rotor) represents the first-time integration of several aligned X-ray exposures and planarizing dielectric steps into a MEMS fabrication process, producing a working, five-layer magnetic motor. While the motor functions, full testing has not been completed.

Process integration was key to successful fabrication of the minimotors. Major problems that were overcome included planarizing dielectric/metal coefficient of thermal expansion mismatch; voids, including those caused by CTE mismatch; residue-free development of small features in thick optically exposed resist and X-ray-exposed PMMA resist up to 300  $\mu$ m thick; and initiation of electrodeposition in all vias. Electrodeposition played a key role in the fabrication of the minimotors; an alternative metal-deposition process is not available for this type of MEMS fabrication.

## **Acknowledgments**

This work was supported in part under Technology Reinvestment Project Development Agreement MDA972-94-3-0043. The authors are grateful to Steve Buchwalter for making available the low-TCE dielectric material. The authors gratefully acknowledge the receipt of X-ray-patterned PMMA samples from R. Wood [Microelectronics Center of North Carolina (MCNC)], and C. Khan Malek, Z. Ling, and Y. Vladimirsky [Center for Advanced Microstructures and Devices (CAMD), Louisiana]. The authors are grateful to S. Roux for mask creation. Finally, the authors wish to acknowledge useful discussions with C. Ahn (University of Cincinnati, Ohio), K. Markus (MCNC), R. Acosta, L. Shi, D. Rath,

D. Herman, J. Gelorme, M. Berkinblitt, and J. Dukovic.

\*\*Trademark or registered trademark of B & D Industrial and Mining Services, Inc., Shell Chemical Company, Union Carbide Corporation, Shipley Company, or Hoechst Celanese Corporation.

#### References

- C. H. Ahn, Y. J. Kim, and M. G. Allen, *IEEE/ASME J. Micromechan. Syst.* 2, No. 4, 165 (1993).
- 2. T. Chainer and L. T. Romankiw, *Proceedings of the Fourth International Symposium on Magnetic Materials and Devices*, L. T. Romankiw and D. Herman, Eds., PV 95-18, The Electrochemical Society, 1996, p. 386.
- 3. P. L. Trouilloud, Ibid., p. 493.
- L. T. Romankiw, in Magnetic Materials, Processes, and Devices, Proceedings of The Electrochemical Society, PV 90-8, 1990, p. 39.
- 5. C. H. Ahn, Y. J. Kim, and M. G. Allen, IEEE/ASME J. Microelectromechan. Syst. (MEMS) 2, No. 4, 165 (1990).
- C. H. Ahn, Y. J. Kim, and M. G. Allen, *IEEE Trans. Components, Hybrids, Manuf. Technol.* 25, No. 3, 356 (1994).
- N. LaBianca and J. D. Gelorme, *Proc. SPIE* 2438, 846 (1995).
- E. E. Castellani, J. V. Powers, and L. T. Romankiw, U.S. Patent 4,102,756, 1979.
- N. C. Anderson and C. R. Grover, Jr., U.S. Patent 4,279,707, 1981.
- J. V. Powers and L. T. Romankiw, U.S. Patent 3,652,442, 1972.
- P. C. Andricacos, M. Branger, R. M. Browne, J. O. Dukovic, B. W. B. Fu, R. W. Hitzfeld, M. Flotta, D. R. McKenna, L. T. Romankiw, and S. Sahami, U.S. Patent 5,312,532, 1994.
- S. Mehdizadeh, J. Dukovic, P. C. Andricacos, L. T. Romankiw, and H. Y. Cheh, J. Electrochem. Soc. 137, 110 (1990).
- S. Mehdizadeh, J. Dukovic, P. C. Andricacos, L. T. Romankiw, and H. Y. Cheh, J. Electrochem. Soc. 139, 78 (1992).
- S. Mehdizadeh, J. Dukovic, P. C. Andricacos, L. T. Romankiw, and H. Y. Cheh, J. Electrochem. Soc. 140, 3497 (1993).
- See for example L. T. Romankiw and E. J. M. O'Sullivan, in Handbook of Microlithography, Micromachining, and Microfabrication, Vol. 2: Micromachining and Microfabrication, P. Rai-Choudhury, Ed., SPIE Optical Engineering Press, Bellingham, WA, 1997, pp. 197–298.
- C. K. Malek, R. Wood, B. Dudley, Z. Ling, and V. Saile, presented at SPIE Micromachining and Microfabrication '96, Microlithography and Metrology in Micromachining II, Austin, TX, October 14–15, 1996.

Received July 10, 1997; accepted for publication June 6, 1998

Eugene J. O'Sullivan IBM Research Division, Thomas J. Watson Research Center, P.O. Box 218, Yorktown Heights, New York 10598 (eosull@us.ibm.com). Dr. O'Sullivan is a Research Staff Member in the Advanced Manufacturing Technology Department. He joined the Research Division in 1984. Dr. O'Sullivan received his Ph.D. in electrochemistry from University College, Cork, Ireland, in 1981. From 1980 to 1983 he was a Postdoctoral Fellow at Case Western Reserve University, and he was a Senior Research Associate at Case from 1983 to 1984. At IBM, Dr. O'Sullivan's research has included fundamental and applied aspects of electroless metal deposition, e.g., diffusion barriers, selectivity of deposition, polyimide adhesion, and new electroless alloy deposition solutions. More recently, he has worked on the fabrication of a multilayer magnetic minimotor. Dr. O'Sullivan is currently working on aspects of MRAM device fabrication for nonvolatile memory application.

Emanuel I. Cooper IBM Research Division, Thomas J. Watson Research Center, P.O. Box 218, Yorktown Heights, New York 10598 (eicooper@us.ibm.com). Dr. Cooper received a Ph.D. degree in chemistry from the Technion (Israel Institute for Technology) in 1981. With C. A. Angell at Purdue University, he investigated organic molten salts, halide glasses, plastic crystals, and ionic conductors. In 1984 he joined the IBM Research Division at the Thomas J. Watson Research Center, where he is currently a Staff Engineer in the Systems, Technology, and Science Department. At IBM he has worked on many chemistry and materials research topics, including macro-defect-free cements, chemistry of high-temperature superconductors, moldable polymer-ceramic composites, analysis of plating and etching baths, and plating of magnetic materials. Dr. Cooper has received three IBM Invention Achievement Awards. He is a member of the American Chemical Society, the Materials Research Society, and the Electrochemical Society.

Lubomyr T. Romankiw IBM Research Division, Thomas J. Watson Research Center, P.O. Box 218, Yorktown Heights, New York 10598 (roman@watson.ibm.com). Dr. Romankiw is an IBM Fellow at the Thomas J. Watson Research Center. He received a B.Sc. in chemical engineering in 1955 from the University of Alberta, and M.Sc. and Ph.D. degrees in metallurgy and materials science in 1962 from the Massachusetts Institute of Technology. Since 1962, when he joined IBM, he has developed dry and electrochemical fabrication processes. He was first to demonstrate patterning by the plating-through-mask technique, which is now the primary method used for patterning thin-film magnetic heads, thin-film packaging, X-ray lithography, C4 plating, and back end-of-line (BEOL) processing. He has made significant contributions to the processes and tools for fabricating magnetic thin-film heads, X-ray lithography masks, bubble memory devices, and the interconnections on integrated circuits and electronic packages. He was the inventor of the currently used merged magnetoresistive (MR)-read inductive write head. He was a coinventor of laser-enhanced plating and etching and of through-mask jet electroetching. Dr. Romankiw has authored or coauthored 47 patents, more than 130 technical papers and reports, and three book chapters, he was an editor of six Electrochemical Society proceedings volumes. He is a member of the Electrochemical Society, the AESF, the International Society of Electrochemistry, the IEEE, the Schevchenko Scientific Society, the Ukrainian Engineers Society, Sigma Xi, and Phi Lambda Upsilon. Dr. Romankiw has received ten IBM Outstanding Invention and Outstanding Contribution Awards and 24 IBM Invention Achievement

Awards. In 1984, together with R. J. von Gutfeld, he received the Research Award from the Electrodeposition Division of the Electrochemical Society. Dr. Romankiw was named a member of the IBM Academy of Technology in 1987 and an ECS Fellow in 1990; he was elected a member of the Academy of Engineering Sciences of Ukraine in 1992. He received the AESF Scientific Achievement Award in 1992, the ACS Distinguished Chemist of Westchester Award and the Perkin Medal in 1993, and the ECS de Vittorio de Nora Medal and Award and the Morris N. Liebman Award from the IEEE in 1994. Dr. Romankiw was listed in Who's Who in America in 1995 and was named an IEEE Fellow in 1996.

Keith T. Kwietniak *IBM Research Division, Thomas J. Watson Research Center, P.O. Box 218, Yorktown Heights, New York 10598 (ktk@us.ibm.com).* Mr. Kwietniak received his B.S. degree in chemistry in 1985 from Pace University, and his M.S. degree in materials science in 1996 from Polytechnic University. He joined the IBM Research Division in 1985 to develop materials and processes for e-beam and X-ray lithography. His work had been primarily concerned with microfabrication of advanced submicrometer CMOS and bipolar semiconductor devices. In 1993 he transferred to the Electrochemical Technology Department, where he is working on applications for plating technology, the analysis of electroplated alloys, and the monitoring and control of electroplating solutions. He is a member of the Electrochemical Society.

Philip L. Trouilloud IBM Research Division, Thomas J. Watson Research Center, P.O. Box 218, Yorktown Heights, New York 10598 (plt@us.ibm.com). Dr. Trouilloud is a graduate of the École Polytechnique in France and received his doctorate from the Laboratoire de Physique des Solides at Orsay, Université Paris XI, France, in 1984. He subsequently studied the magnetic properties of thin metallic films in the Electrical Engineering Department at the University of Texas at Austin. Since 1987, he has worked on the characterization of magnetic devices, with special emphasis on Kerr imaging techniques, at the IBM Thomas J. Watson Research Center. He is currently involved with the study of magnetic tunnel junctions for memory and sensor devices.

Jean Horkans 1BM Research Division, Thomas J. Watson Research Center, P.O. Box 218, Yorktown Heights, New York 10598 (horkan@us.ibm.com). Dr. Horkans is a Research Staff Member at the IBM Thomas J. Watson Research Center working in the field of microelectronics manufacturing research. Her main interests are electrochemistry and electrodeposition. She joined IBM at the Watson Research Center in 1973 after having received a B.A. in chemistry from St. Olaf College and a Ph.D. in chemistry from Case Western Reserve University. She received an IBM Outstanding Technical Achievement Award in 1982 for development of electrochemical monitors and a Research Division Award in 1991 for contributions to magnetic disks. Dr. Horkans is a member of the Electrochemical Society and the New York Academy of Sciences.

Christopher V. Jahnes *IBM Research Division, Thomas J. Watson Research Center, P.O. Box 218, Yorktown Heights, New York 10598 (jahnes@us.ibm.com).* Mr. Jahnes joined *IBM in 1983 after completing his A.A.S. degree in electrical* 

engineering technology at Rockland Community College. He is currently a Staff Engineer in the Plasma Process group, working on the integration of low-dielectric-constant materials for semiconductor interconnect technologies. His research interests include plasma processing and materials engineering for semiconductor and storage applications. He has received six IBM Invention Achievement Awards and holds six patents.

Inna V. Babich IBM Research Division, Thomas J. Watson Research Center, P.O. Box 218, Yorktown Heights, New York 10598 (inna@us.ibm.com). Ms. Babich received her M.S. degree in chemistry and chemical engineering from the Institute of Chemical Technology, Moscow, Russia. She worked at the Russian Academy of Science in the field of organosilicon chemistry. In 1984, she joined the IBM Thomas J. Watson Research Center and worked on development of X-ray masks and other processes for proximity X-ray lithography. In 1995 Ms. Babich worked on development of single-layer and multilayer positive-resist processes utilizing optical lithography for a micromotor program. She is currently a member of the Advanced Deep UV Lithography group, working on process development of sub-180-nm critical dimensions.

Sol Krongelb IBM Research Division, Thomas J. Watson Research Center, P.O. Box 218, Yorktown Heights, New York 10598 (kron@us.ibm.com). Dr. Krongelb received a B.S. degree in engineering physics from New York University, College of Engineering, and the M.S. and Ph.D. degrees in physics from the Massachusetts Institute of Technology. He joined IBM in 1958 at the Thomas J. Watson Research Center and has spent the major part of his career developing device fabrication technology which combines electrodeposition with the more traditional lithographic, wet and dry etching, and vacuum deposition processes. Dr. Krongelb played a significant role in the development of the thin-film magnetic recording head fabrication process and subsequently in the introduction of plating technology to highend package fabrication. In 1993, Dr. Krongelb retired from IBM as Manager of Device Fabrication and Patterning but has continued to pursue his technical interests as a Research Staff Member Emeritus at the Thomas J. Watson Research Center. His recent activities have included developing new fabrication processes for fabricating MEMS structures. Dr. Krongelb is a member of the American Vacuum Society, the Electrochemical Society, and the Institute of Electrical and Electronics Engineers.

Suryanarayan G. Hegde IBM Research Division, Thomas J. Watson Research Center, P.O. Box 218, Yorktown Heights, New York 10598 (hegde@us.ibm.com). Dr. Hegde is a Research Staff Member at the IBM Thomas J. Watson Research Center. He is currently involved in advanced DRAM development in the IBM Microelectronics Division. Since joining the IBM Research Division in 1982, Dr. Hegde has contributed to various aspects of direct-access storage technology, including advanced actuator designs, head-disk interface tribology, and magnetic media. He received a Ph.D. degree in physics from Stevens Institute of Technology in 1979. Prior to joining IBM, Dr. Hegde was a member of the physics faculty at Rutgers University.

James A. Tornello IBM Research Division, Thomas J. Watson Research Center, P.O. Box 218, Yorktown Heights, New York 10598 (tornello@us.ibm.com). Mr. Tornello is currently working in the Planarization Technology group in the Semiconductor Physics and Devices Department at the Thomas J. Watson Research Center. He received his B.A. in physics in 1977 at SUNY-College at Oswego and his M.S. in metallurgical engineering in 1986 at Polytechnic University. Mr. Tornello joined the IBM Research Division in 1978, working in the area of semiconductor science and technology, helping to develop and test novel devices in advanced semiconductor physics. He worked with a group that designed and built a small semiconductor fabrication facility, becoming a process technologist with technical expertise in oxidation, RIE, LPCVD, metallization, and, in particular, lithography, including mask design. He later worked on Dr. Romankiw's team, which developed thin-film multilevel wiring alternatives using electrodeposition-through-resist technology. Mr. Tornello became interested in microelectromechanical systems (MEMS) and collaborated with the team which developed the process technology needed to build the integrated variablereluctance minimotor. He is currently working in the area of chemical-mechanical planarization (CMP) in the Planarization Technology group.

Nancy C. LaBianca IBM Research Division, Thomas J. Watson Research Center, P.O. Box 218, Yorktown Heights, New York 10598 (labianca@us.ibm.com). Ms. LaBianca is a Staff Engineer in the Applied Polymer Technology group at the Thomas J. Watson Research Center. She joined IBM in 1988, working to develop gate-metal processes for GaAs technology. She then joined her current group, where she has contributed to a broad range of lithographic activities, including highresolution photosensitive polyimides for advanced multichip packaging, and the current negative resist, CGR, that is used in manufacturing IBM logic chips. She is currently involved in the imaging of very thick films for micromachining applications; her work in this area has been published and presented at the SPIE and the ECS. Ms. LaBianca is a member of the International Society of Photo-Optical Instrumentation Engineers (SPIE).

John M. Cotte IBM Research Division, Thomas J. Watson Research Center, P.O. Box 218, Yorktown Heights, New York 10598 (cotte@us.ibm.com). Mr. Cotte received a B.S. degree in chemical engineering from Bucknell University in 1984, and an M.S. degree in materials science and engineering from the University of Pittsburgh in 1988. He joined the IBM Research Division in 1988 and worked in the Physical Sciences Analytical Department on analysis of electronic materials by SIMS. In 1993 he joined the Electrochemical Technology Department, where he was involved in materials characterization utilizing electron-beam techniques. He currently works in the Flip-Chip Interconnect Department on the development of electrochemically fabricated C4s.

Timothy J. Chainer IBM Research Division, Thomas J. Watson Research Center, P.O. Box 218, Yorktown Heights, New York 10598 (tchainer@us.ibm.com). Dr. Chainer is Manager of the Storage Instrumentation and Measurements group at the IBM Thomas J. Watson Research Center. Since joining IBM

in 1981, he has worked in the areas of magnetic storage, manufacturing research, and signature verification. His work has included the development of a flexural actuator for tape drives, methods of disk file servowriting, and the design of a pen transducer and algorithms for biometric identification. He has received three IBM Outstanding Technical Achievement Awards, holds 15 U.S. patents, and is the author of 12 scientific papers. Dr. Chainer received a B.S. in engineering science in 1973 and a Ph.D. in physics from Rutgers University in 1980. He is a Senior Member of the IEEE and a member of the American Physical Society.